



ELSEVIER

Journal of Nuclear Materials 266–269 (1999) 761–765

Journal of  
nuclear  
materials

# Deuterium transport in Cu, CuCrZr, and Cu/Be

R.A. Anderl<sup>a,\*</sup>, M.R. Hankins<sup>a</sup>, G.R. Longhurst<sup>a</sup>, R.J. Pawelko<sup>a</sup>

<sup>a</sup> Fusion Safety Program, Idaho National Engineering and Environmental Laboratory, Lockheed Martin Idaho Technologies Company, P.O. Box 1625, Idaho Falls, ID 83415-7113, USA

## Abstract

This paper presents the results of deuterium implantation/permeation experiments and TMAP4 simulations for a CuCrZr alloy, for OFHC-Cu and for a Cu/Be bi-layered structure at temperatures from 700 to 800 K. Experiments used a mass-analyzed, 3-keV  $D_2^+$  ion beam with particle flux densities of  $5 \times 10^{19}$  to  $7 \times 10^{19}$  D/m<sup>2</sup> s. Effective diffusivities and surface molecular recombination coefficients were derived giving Arrhenius pre-exponentials and activation energies for each material: CuCrZr alloy, ( $2.0 \times 10^{-2}$  m<sup>2</sup>/s, 1.2 eV) for diffusivity and ( $2.9 \times 10^{-14}$  m<sup>4</sup>/s, 1.92 eV) for surface molecular recombination coefficients; OFHC Cu, ( $2.1 \times 10^{-6}$  m<sup>2</sup>/s, 0.52 eV) for diffusivity and ( $9.1 \times 10^{-18}$  m<sup>4</sup>/s, 0.99 eV) for surface molecular recombination coefficients. TMAP4 simulation of permeation data measured for a Cu/Be bi-layer sample was achieved using a four-layer structure (Cu/BeO interface/Be/BeO back surface) and recommended values for diffusivity and solubility in Be, BeO and Cu. © 1999 Elsevier Science B.V. All rights reserved.

**Keywords:** First wall materials; Ion implantation; Deuterium transport; Permeation; Diffusion

## 1. Introduction

Quantification of tritium uptake, retention and permeation in plasma-facing component (PFC) materials is important to the assessment of safety issues for large-scale tokamaks such as the International Thermonuclear Experimental Reactor (ITER) [1]. Analytical models that are used to predict these quantities require accurate transport information, such as diffusivity, solubility and surface molecular recombination data for the materials. Reviews of the hydrogen transport data base for fusion-relevant materials have been reported recently by Reiter et al. [2] and by Dolan and Anderl [3], and they point to a lack of transport data for copper alloys proposed as substrates in ITER bi-layer PFC structures in which Be is bonded to a copper-alloy substrate. The purpose of this paper is to twofold: (1) to experimentally determine diffusivity and surface molecular recombination data for an ITER-relevant CuCrZr alloy and for pure copper at comparable test conditions and (2) to investigate the transport of deuterium through bi-layer structures of Be

and Cu by experiment and model simulation calculations with the TMAP4 code [4]. A more detailed presentation of this work has been issued as an internal report [5].

## 2. Experimental details

Our approach involved deuterium implantation/permeation experiments for thin, 2.54 cm diameter specimens of CuCrZr, Cu and Cu/Be bi-layer specimens in the temperature range 700 to 800 K. CuCrZr specimens were machined from AMPCOLOY 972 alloy bar stock (98.7% Cu, 1.1% Cr, 0.1% Zr), with final mechanical polishing to a mirror finish and a thickness of 0.064 cm. Cu test specimens were machined from oxygen-free-high-conductivity (OFHC) Cu flat stock, with final mechanical polishing to a mirror finish and a thickness of 0.064 cm.

Cu/Be bi-layer specimens were fabricated by Argon/sputter-deposition of copper coatings onto high purity foils of Be heated to 673 K during the deposition. The Be substrate material was Electrofusion type IF-1 foil (extruded and hot-rolled, ingot metallurgy cast material produced from vacuum-melted, electrolytically-refined

\* Corresponding author. Tel.: +1-208 533 4153; fax: +1-208 533 4207; e-mail: raa@inel.gov

Be flakes of 99.96% Be) that was mechanically polished to a mirror finish and a thickness of 55  $\mu\text{m}$  prior to coating with copper. Specimens with 1  $\mu\text{m}$  and 5  $\mu\text{m}$  thick copper coatings were prepared, with the 1  $\mu\text{m}$  sample used for permeation studies and the 5  $\mu\text{m}$  sample used for annealing studies. Depth-profile Auger analysis of the as-prepared, 1  $\mu\text{m}$  Cu/Be specimen revealed a bulk composition in the coating of 73% Cu, 19% Be, 6% O and 2% C. After heating the 1  $\mu\text{m}$  Cu/Be specimen at 700 K for about 3 h during two implantation/permeation experiments, bulk composition of the coating outside the beam exposure area changed to 58% Cu, 28% Be, 9% O and 3% C, and the surface was enriched to about 60% Be. In the beam-exposure area, the composition changed to 33% Cu, 51% Be, 10% O, and 6% C, with Cu reduction and Be enhancement attributed to some sputter erosion of the Cu coating.

Ion implantation/permeation experiments used a mass-analyzed, 3 keV  $\text{D}_3^+$  ion beam in a system described previously [6,7]. Flux densities for the nominal 1 keV/D implanting ions ranged from  $5 \times 10^{19}$  to  $7 \times 10^{19}$   $\text{D}/\text{m}^2 \text{ s}$  through a 20  $\text{mm}^2$  beam-defining aperture. Foil specimens were mounted in the target assembly by sandwiching them between two flanges with aluminum gaskets that sealed against the foil upstream (US) and downstream (DS) surfaces. Specimen temperatures were based on thermocouple measurements of the support-flange temperature. Deuterium re-emission and permeation data were based on time-sequenced measurements of the mass-4 peaks, as observed with quadrupole mass spectrometers (QMS) in the US and DS vacuum chambers. Each QMS was calibrated with deuterium standard leaks. Vacuum system base pressure was 1  $\mu\text{Pa}$ .

### 3. Measurements, analyses and results

Implantation/permeation experiments were performed at temperatures of 700–780 K for CuCrZr, 710–785 K for Cu, and 700 K for the 1  $\mu\text{m}$  Cu/Be bi-layer specimen. Each experiment entailed at least two beam-on/beam-off segments, and ion-exposure was continued for sufficient time to assure nominal steady-state conditions at which the measured permeation and re-emission signals were constant for a constant incident ion flux.

Representative examples of measured permeation data for CuCrZr and Cu at 730 K are shown in Figs. 1 and 2, respectively. In these figures, the measured permeation flux is plotted as a function of time, with time zero corresponding to the beam-on time and with a beam-off time of about 120 min that correlates with the fall-off in the permeation signal. Discussion of the open circle data corresponding to TMAP4 simulations is deferred to a later paragraph.

Effective diffusivity values were derived from the measured permeation data by two analysis approaches:

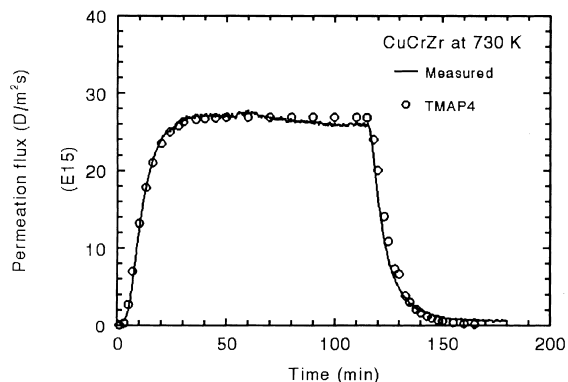


Fig. 1. Permeation data measured for CuCrZr at 730 K and exposed to an ion flux of  $6.4 \times 10^{19}$   $\text{D}/\text{m}^2 \text{ s}$  for 114 min. Open circles correspond to a TMAP4 simulation calculation, based on diffusivity and molecular recombination values that were derived in this work.

(1) lag-time analysis [8] applied to the initial beam-on portion of the permeation data and (2) fitting of the evolution data that follows the beam-off time. Both approaches hinge on diffusion-limited transport in the material, a condition that is met for these experiments. Permeation lag-times,  $t_l$ , were derived as the time-axis intercepts of the steepest tangents to the initial beam-on segments of the permeation data. As shown by Longhurst et al. [8], diffusivity can then be computed using Eq. (1):

$$2t_l = \tau = L^2/(\pi^2 D), \quad (1)$$

where  $\tau$  is defined as the characteristic diffusion time,  $L$  is the specimen thickness and  $D$  is the diffusivity. The second method for deriving effective diffusivities from

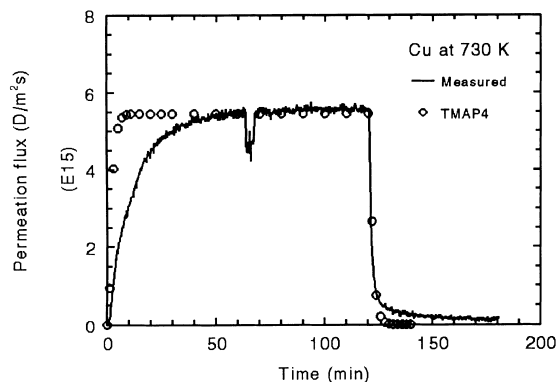


Fig. 2. Permeation data measured for OFHC-Cu at 730 K and exposed to an ion flux of  $7.1 \times 10^{19}$   $\text{D}/\text{m}^2 \text{ s}$  for 120 min. Open circles correspond to a TMAP4 simulation calculation, based on diffusivity and molecular recombination values that were derived in this work.

the permeation data is based on fitting Eq. (2) to the evolution data:

$$J_p = (c_1 D/L) \{1 + 2 \sum [(-1)^m \exp(-m^2 t/\tau)]\}. \quad (2)$$

In Eq. (2), the sum of the exponential terms goes from 1 to infinity, but usually only 6 terms are required to produce an adequate representation of the evolution transient. Adjustable parameters in the fit are  $c_1$  and the characteristic time,  $\tau$ . Diffusivities are computed using Eq. (1), once a fit value for  $\tau$  is determined.

Fig. 3 compares literature-recommended diffusivity values (Cu-Reiter) for pure Cu [2] with effective diffusivity values for CuCrZr and OFHC-Cu, as derived by the lag-time (LT) approach and the evolution transient (Fit) approach in these experiments. For CuCrZr, the LT- and FIT-derived diffusivity values are in reasonable agreement, whereas, for OFHC-Cu, the Fit values are considerably higher. We believe that this discrepancy is associated with phenomena giving rise to the non-classical shape of the beam-on portion of the permeation curve for Cu, as observed in Fig. 2. For a true diffusion-limited condition, the injection portion of the curve should be a mirror reflection of the evolution portion of the curve, a feature manifested by the CuCrZr data for most of the test temperatures. However, as pointed out in other work on tungsten [9], we believe that this deviation is due to the influence of strong bulk trapping that varies spatially with time until trap saturation occurs and to an upstream surface molecular recombination rate that varies spatially with time, both effects that are related to ion exposure with a 2D Gaussian-shaped beam. These effects, primarily observed for samples with high lattice diffusivity, could cause the injection transient to rise more slowly than that expected based on the

lattice diffusivity. Hence, the lag-time approach may be unacceptable for deriving diffusivities for OFHC-Cu. However, these effects have little impact on the evolution transient, so diffusivities based on this approach are more accurate. The straight lines through the diffusivity data plotted in Fig. 3 correspond to fits of an Arrhenius expression to each of the respective data sets with pre-exponentials and activation energies as follows: Cu-Fit ( $2.1 \times 10^{-6}$  m<sup>2</sup>/s, 0.52 eV), CuCrZr-Fit ( $2.0 \times 10^{-2}$  m<sup>2</sup>/s, 1.2 eV), and Cu-Reiter ( $8.0 \times 10^{-7}$  m<sup>2</sup>/s, 0.387 eV).

Surface molecular recombination coefficients were obtained from the measured permeation data using two approaches. Estimates of the upstream surface molecular recombination coefficient,  $K_r$ , were derived using Eq. (3), because the re-emission flux,  $J_r$ , the permeation flux,  $J_p$ , the diffusivity,  $D$ , the sample thickness,  $L$ , and the range,  $R$ , of implanting ions are known:

$$K_r = (D^2/2L^2)(J_r/J_p^2)(1 - (R/L)(J_r/J_p))^{-2}. \quad (3)$$

In addition,  $K_r$  values were refined by using TMAP4 simulation calculations to fit the entire measured permeation curve. Input for this approach included the following: specimen thickness, implantation fluxes corresponding to the specific experiment and distributed at the mean range location, effective diffusivities obtained from the previous evolution transient ‘Fit’ analyses, and initial  $K_r$  estimates derived using Eq. (3). Usually, to achieve a reasonable fit to the permeation curve, the magnitude of  $K_r$  was adjusted slightly from the initial estimate to achieve a match between the calculated curve and the steady-state permeation level.

Figs. 1 and 2 show examples of TMAP4 calculational fits to the measured permeation data for CuCrZr and OFHC-Cu at 730 K, respectively. The TMAP4 simulation of the permeation curve is excellent for CuCrZr, whereas the TMAP4 simulation for OFHC-Cu matches the steady-state permeation level and the evolution transient but deviates somewhat from the measured injection (beam-on) transient. As discussed previously, we believe that this deviation is due to the influence of strong bulk trapping that varies spatially with time until trap saturation occurs and to an upstream surface molecular recombination rate that varies spatially with time, both effects that are related to ion exposure with a 2D Gaussian-shaped beam. Such effects are not simulated in the 1D TMAP4 code. The effects are more pronounced for temperatures at which lattice diffusivity is high, the case for all Cu test temperatures and for only the highest temperatures for CuCrZr.

A summary of the derived surface molecular recombination coefficients is presented in Fig. 4. For comparison, recombination coefficient values shown by the solid line correspond to pure copper values that were computed using the Baskes formalism [10], with recommended Cu diffusivity and solubility parameters [2,3] used in the calculations. These results demonstrate a

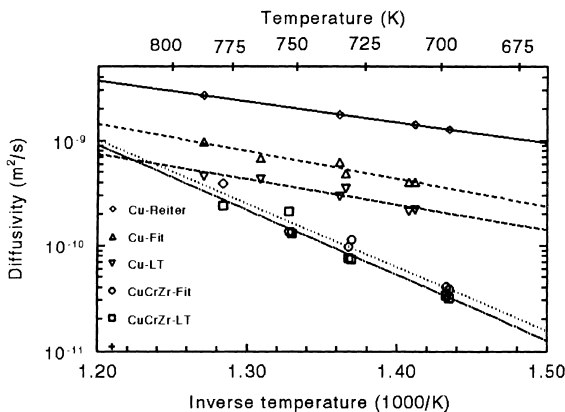


Fig. 3. Arrhenius plots of effective diffusivities that were derived from measured permeation data for CuCrZr-alloy and OFHC-Cu using the lag-time (LG) method and a series exponential (Fit) to the evolution transients of the permeation data. Literature-recommended values [2] for diffusivity in pure Cu are shown by the data identified as Cu-Reiter.

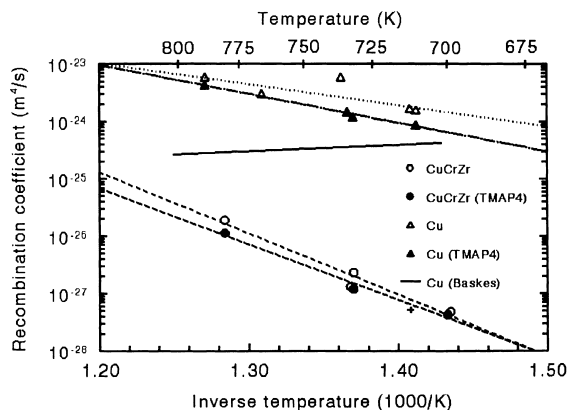


Fig. 4. Arrhenius plots of surface molecular recombination coefficients that were derived from measured permeation data for CuCrZr-alloy and OFHC-Cu using Eq. (9) and TMAP4 simulation calculations that matched the permeation data. Recombination values estimated using the Baskes formalism [10] for pure copper are shown for comparison.

large difference in surface molecular recombination values for pure Cu compared to CuCrZr alloy. The straight lines through the recombination data plotted in Fig. 4 correspond to fits of an Arrhenius expression to each of the respective data sets, with pre-exponentials and activation energies for the TMAP4 cases as follows: CuCrZr ( $2.9 \times 10^{-14} \text{ m}^4/\text{s}$ , 1.92 eV), and OFHC-Cu ( $9.1 \times 10^{-18} \text{ m}^2/\text{s}$ , 0.99 eV).

Fig. 5 presents permeation results for the 1  $\mu\text{m}$  Cu/55  $\mu\text{m}$  Be bi-layer specimen exposed at 700 K on the Cu side to an incident flux of  $5.6 \times 10^{19} \text{ D}/\text{m}^2 \text{ s}$  for 100 min. The solid curve corresponds to a five-point smoothing of the measured data that show a lot of scatter. The open circles correspond to permeation data calculated with a TMAP4 simulation of the layered specimen modeled as a four material region consisting of the following: 1  $\mu\text{m}$  Cu/0.001  $\mu\text{m}$  BeO interface/55  $\mu\text{m}$  Be bulk/0.02  $\mu\text{m}$  BeO

back surface. Transport data for the Be, BeO and Cu that were used as input to this calculation corresponded to literature-recommended values for diffusivity ( $D$ ) and solubility ( $S$ ) for these materials [2,3]. Surface recombination coefficients for BeO and Cu were assumed to be the following:  $4.5 \times 10^{-30} \text{ molecule-m}^4/\text{atom}^2 \text{ s}$  for BeO and  $2.1 \times 10^{-26}$ – $4.3 \times 10^{-25} \text{ molecule-m}^4/\text{atom}^2 \text{ s}$  for Cu. The simulation calculation provides a reasonable fit to the measured permeation level and the evolution transient, with some deviation between the measured and calculated data for the injection transient.

#### 4. Concluding remarks

Implantation/permeation experiments and TMAP4 simulation calculations were performed to obtain deuterium transport data for Ampcoloy 972, a CuCrZr alloy, and for OFHC-Cu. Measured permeation rates for comparable thickness specimens and implanting deuterium fluxes were about a factor of 5 higher in CuCrZr than in OFHC-Cu at temperatures from 700–785 K. Derived diffusivities were much smaller in CuCrZr than in OFHC-Cu for temperatures between 700–785 K. This could be due to trapping at alloying elements such as Zr [11–14]. Derived surface molecular recombination coefficients were significantly smaller for CuCrZr than for OFHC-Cu at temperatures from 700–785 K, resulting in enhanced permeation in CuCrZr. TMAP4 calculations provided an excellent simulation of the measured permeation data for CuCrZr. Derived diffusivities were about a factor of three smaller than recommended values [2,3] for Cu at temperatures from 700–785 K, indicating the possibility of some trap-delayed diffusion by beam-induced or fabrication-related defects in the test specimens. Measured permeation data deviated from TMAP4 simulation in the initial beam-on part of the permeation curve for Cu, indicating the possible influence of spatially-varying, strong bulk trapping and

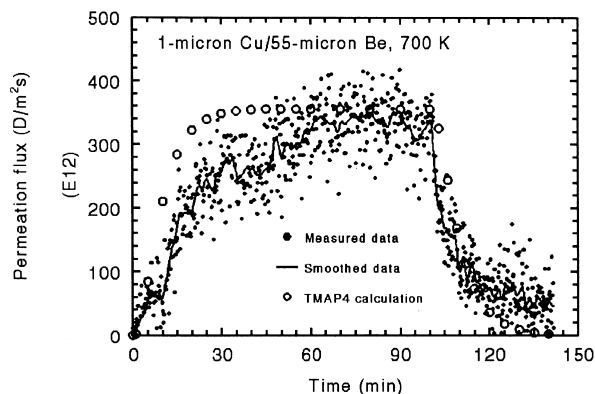


Fig. 5. Permeation results for the 1  $\mu\text{m}$  Cu/55  $\mu\text{m}$  Be bi-layer specimen exposed at 700 K on the Cu side to an incident flux of  $5.6 \times 10^{19} \text{ D}/\text{m}^2 \text{ s}$  for 100 min.

spatially-varying, upstream surface molecular recombination rates resulting from ion exposure with a 2D Gaussian-shaped ion-beam profile. TMAP4 calculations provided an excellent simulation of the steady-state permeation and the evolution transient portion of the Cu permeation data

Implantation/permeation experiments and TMAP4 simulations were done to investigate deuterium transport through bi-layer structures of Cu and Be. For deuterium implantation into the Cu coating of a 1- $\mu\text{m}$ Cu/55  $\mu\text{m}$  Be bi-layer specimen at 700 K, measured permeation rates were much less than through thicker specimens of pure Cu. TMAP4 simulation of the measured permeation data was achieved using currently recommended values for diffusivity and solubility in Cu, Be, and BeO, assuming realistic thicknesses of a BeO interface between the Cu and the Be substrate and of the BeO layer on the specimen backside. Systematic studies [5] in which the BeO thicknesses were varied in the TMAP4 calculations demonstrated a high sensitivity of the calculated permeation rates to changes in the BeO layer thickness, especially at the Cu/Be interface.

Based on the results of this work, we recommend the following for future research: (1) systematic studies to investigate the influence of alloying elements and fabrication processes on the diffusivity and permeability of copper alloys for tokamak plasma-facing component applications and (2) experimental and model simulation studies for Be/Cu bi-layer structures exposed to ITER-relevant plasma fluxes and fluences to determine the influence of surface, bulk and interface effects on deuterium/tritium uptake, retention and permeation.

### Acknowledgements

This work was supported by the US Department of Energy, Director of Energy Research, Office of Fusion Energy Sciences, under DOE Contract DE-AC07-94ID13223.

This report is an account of work assigned to the U. S. Home Team under Task Agreement No. S 81 TT 14

within the Agreement among the European Atomic Energy Community, the Government of Japan, the Government of the Russian Federation, and the Government of the United States of America on Cooperation in the Engineering Design Activities for the International Thermonuclear Experimental Reactor (“ITER EDA Agreement”) under the auspices of the International Atomic Energy Agency (IAEA). The report has not been reviewed by the ITER Publications Office.

### References

- [1] A.E. Poucet, H.W. Bartels, S.J. Piet, Safety analysis guidelines for NSSR1, Ver 1.1, Internal Report S81R1195-12-13 W2, ITER Engineering Design Activity, San Diego, CA, March, 1996.
- [2] F. Reiter, K.S. Forcey, G. Gervasini, A compilation of tritium-material interaction parameters in fusion reactor materials, EUR 15217 EN 1993.
- [3] T.J. Dolan, R.A. Anderl, Assessment of database for interaction of tritium with ITER plasma facing materials, ITER US Home Team Report: ITER/US/94/TE/SA-10, Idaho National Engineering Laboratory Report EGG-FSP-11348, September, 1994.
- [4] G.R. Longhurst et al., TMAP4 User’s Manual, EGG-FSP-10315, Idaho National Engineering Laboratory, June 12, 1992.
- [5] R.A. Anderl et al., Deuterium implantation studies for Cu, CuCrZr-alloy and Cu/Be composites, ITER US Home Team Report: ITER/95/TE/Sa-4 (Rev. 1), Idaho National Engineering Laboratory, May, 1995.
- [6] D.F. Holland, R.A. Anderl, Fusion Technol. 14 (1988) 707.
- [7] R.A. Anderl et al., Fusion Technol. 8 (1985) 2299.
- [8] G.R. Longhurst et al., Fusion Technol. 19 (1991) 1799.
- [9] R.A. Anderl et al., Fusion Technol. 21 (1992) 745.
- [10] M.I. Baskes, J. Nucl. Mater. 92 (1980) 318.
- [11] Yu.I. Belyakov, Yu.I. Ebezdin, Uch. Zap. Leningrad. Gos. Univ. Ser. Fiz. Nauk. 345 (1968) 44, National Bureau of Standards publication PB-250 (1974) 833 Eng. translation.
- [12] D.R. Begeal, J. Vac. Sci. Technol. 15 (3) (1978) 1146.
- [13] D.J. Mitchell, J. Vac. Sci. Technol. 20 (4) (1982) 1048.
- [14] D.J. Mitchell et al., J. Appl. Phys. 53 (2) (1982) 970.